

North Atlantic Space Weather Characterizing the Space Radiation Environment of Transatlantic Flights and Estimating Radiation Exposure to Commercial Crew

Spring 2025 | Virginia – Langley
August 8th, 2025

Authors: Tanya Kasyanchuk (Analytical Mechanics Associates), Sarah Schneider (Analytical Mechanics Associates), Satwika Tattari (Analytical Mechanics Associates), Will Warden (Analytical Mechanics Associates)

Abstract:

Significant space weather events cause increased radiation exposure within the Earth's atmosphere at aviation altitudes, impacting the physical health of pilots, air crew, and passengers. Repeated or extreme radiation exposure can lead to an increased risk of cancer, cataracts, and other health issues. The tracking of space weather events and radiation levels aid pilots in making informed decisions of flight altitudes to create the safest path for all crew and passengers on the plane. NASA DEVELOP partnered with the Allied Pilots Association (APA) to observe and visualize the radiation environments on transatlantic routes for three different case studies of significant solar energetic particle (SEP) events. Pilots currently rely on terrestrial weather data for ensuring safety during flights but lack access to space weather information about radiation levels. Using data produced by the Nowcast of Aerospace Ionizing RAdiation System model (NAIRAS), the team plotted radiation environments over varying latitudes and altitudes over the duration of these SEP events. Through mapping the total effective radiation dose and completing quantitative analysis, the team found that changing the altitude of a flight was the most effective way to reduce radiation exposure. These visuals and analyses can provide the APA with data that aids their route planning for better safety on transatlantic flights.

Key Terms:

space weather, radiation, NAIRAS, commercial flight, aviation, total effective dose rate

Advisors: Dr. Xia Cai (NASA Langley Research Center), Dr. Christopher Mertens (NASA Langley Research Center), Dr. Guillaume Gronoff (NASA Langley Research Center), Dr. Daniel Phoenix (NASA Langley Research Center)

Lead: Jack Graziano (Virginia – Langley)

1. Introduction

The Earth's magnetic field and atmosphere actively shield humans from harmful cosmic radiation, but solar energetic particles (SEPs) originating from the Sun and galactic cosmic rays (GCRs) from outside the solar system can sometimes penetrate the atmosphere and cause significant radiation exposure (Mertens et al., 2008). The radiation intensity is increased during notable space weather events. Furthermore, vulnerable populations such as aircraft pilots, flight crew, and pregnant individuals are uniquely exposed to the effects of this radiation. Currently, pilots experience radiation equivalent to around double the annual background radiation dose level encountered by the general population (Langner et al., 2003). The International Commission on Radiological Protection recommends that aircrews do not exceed 20 millisieverts (mSv) per year averaged over 5 years, but this limit drops to 0.5 mSv for pregnant individuals (Xue et al., 2024). For context, 20 mSv is equivalent to 200 chest x-rays and 0.5 mSv is equivalent to 5 chest x-rays considering one x-ray is around 0.1 mSv (Harvard Health Publishing, 2021). Tracking radiation is important to ensure people stay below the limit, especially if they are exposed to high radiation levels. Mertens et al. (2010) found that ignoring geomagnetic storm effects during SEP events can underestimate the radiation exposure at high latitudes from 15% to over 200%. Accordingly, radiation effects from space weather events are of high priority to study for pilots and other parties at risk.

Currently, pilots receive real-time updates on terrestrial weather events during flights, but they do not have space weather information integrated into their systems to change flight paths accordingly to avoid extreme radiation exposure. NASA DEVELOP partnered with the Allied Pilots Association (APA) to help pilots better understand radiation from space weather. This feasibility study used NASA Earth observations to provide pilots with a better understanding of the radiation environment at different aviation altitudes during space weather events. The association serves as the American Airlines Pilots' Union and strives to improve working conditions and environments for pilots. The APA dedicates more than 20% of its income to ensuring and promoting aviation safety (Allied Pilots Association, 2023) and hopes to use DEVELOP's work to further support pilots. For this study, the interests of the APA relate to radiation that pilots, flight crew, and passengers receive when flying through areas of high risk such as polar or high latitude routes. The organization aims to eventually give pilots space weather predictions with a 1-minute temporal resolution to help with rerouting during high radiation events. This study focused on using a preliminary data analysis of past space weather events to help model the space radiation environment. With a model of the space environment from past events, APA can guide pilots in understanding regions of higher radiation risk and planning flight paths while considering radiation risks.

The project primarily focused on the North Atlantic passage specifically, between 40 and 70 degrees latitude since flights commonly pass through this region between New York City and London, and radiation increases at higher latitudes due to changes in the cutoff rigidity (Figure 1). The cutoff rigidity, defined as the amount of shielding the Earth's magnetic field provides from the high energy particles, usually increases with decreasing geomagnetic latitudes (Jun et al., 2024), meaning more energetic particles can enter the Earth's atmosphere at higher latitudes. Due to the shape of the Earth's magnetosphere, the converging magnetic field lines at the poles cause less shielding from radiation at higher latitudes. The radiation from these particles can affect high/mid latitudes depending on the strength of the storm and put commercial flights at risk of elevated radiation exposure. For this study, the team focused on 3 space weather events: the Halloween 2003 storm (October 28, 2003), the storm on January 20, 2005, and the Gannon storm on May 10-11, 2024. These case studies were examples of increased radiation in Earth's atmosphere due to solar activity leading to greater risk to passengers and pilots in the air.

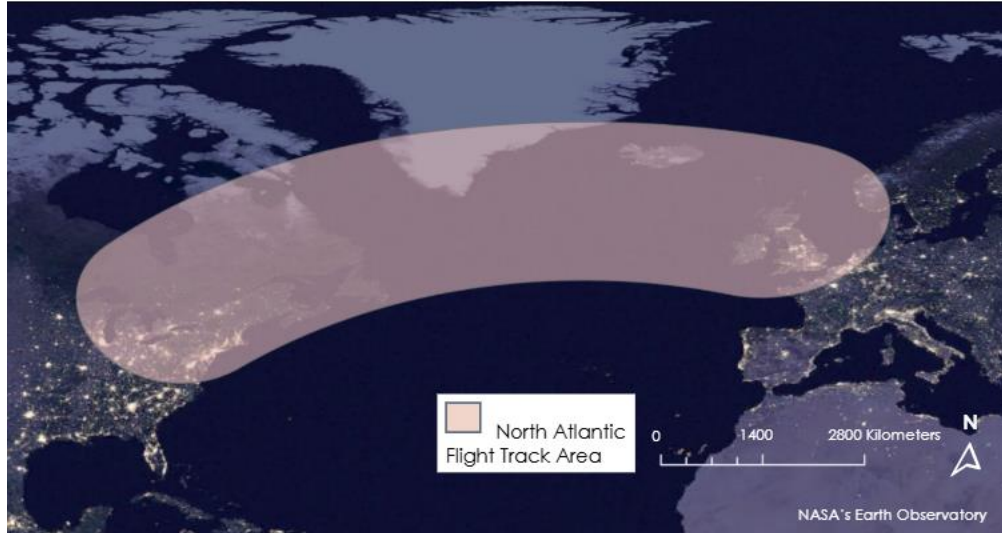


Figure 1: Study area map depicting the North Atlantic. This highlighted area shows the main flight area between 40° - 70° degrees latitude.

The team relied on remote sensing data throughout the project to better understand the levels of radiation observed at higher altitudes and latitudes. This feasibility study aimed to determine whether the Nowcast of Aerospace Ionizing Radiation System (NAIRAS) (NAIRAS model can effectively convey radiation information to pilots for informed decision-making and to communicate information to a broader general audience for educational purposes. NAIRAS is an application of Earth system science results that utilizes a number of different satellites, including sensors onboard Advanced Composition Explorer (ACE), Deep Space Climate Observatory (DSCOVR), and Geostationary Operational Environmental Satellite (GOES).

This study included multiple project objectives. One main objective was to analyze radiation for specific flight paths to better understand how specific routes can affect radiation exposure for pilots. Another objective was to visualize regional and global radiation doses to effectively portray radiation levels in different places around the world. Furthermore, the team wanted to quantitatively analyze the total effective radiation (TED) rates to emphasize the comparison of the radiation exposure to thresholds set by the APA. Additionally the team communicated the information from the project to pilots in an engaging and effective way through the creation of a short video. These outputs demonstrate to pilots the levels of radiation at higher flight altitudes during solar storm events and have the potential to aid in planning future mitigation strategies.

2. Methodology

2.1 Data Acquisition

The team used Version 3 of the NAIRAS model, which provides Level 4 data products through the Community Coordinated Modeling Center (CCMC) to study the radiation environment during space weather events. NAIRAS integrates satellite observations and ground measurements to model Earth's radiation exposure and is able to account for both GCR and SEP radiation.

Satellite inputs to the model include data from ACE and DSCOVR. Instruments from these satellites including, ACE's Electron, Proton, and Alphas Monitor and DSCOVR's Faraday Cup and Magnetometer, provide important measurements of the solar wind density, velocity, and the interplanetary magnetic field (IMF). GOES Energetic Particle Sensor also contributes with measurements of the differential and integral charged particle flux, used to derive the incident solar energetic particles (SEP) spectral fluence rates and calculate radiation dosages. The Earth observations are organized in a table below for reference (Table 1). Additionally, the model uses ground based observations from neutron monitors located globally in Oulu,

Lomnicky, Thule, and Izmiran to compute GCRs and the fluxes of the Earth's inner proton belt. The model also uses Wilcox Solar Observatory (WSO) solar polar magnetic field data to calculate GCRs over time. The solar radio flux at wavelength of 10.7 cm (F10.7) also measures the radio flux over the solar cycles. These combined measurements allow the model to produce radiation estimations from both GCRs and SEPs.

Table 1

Satellite observations used by the NAIRAS model

Platform & Sensor	Parameters	Use
ACE Electron, Proton, and Alpha Monitor (EPAM)	Solar wind velocity, density, and interplanetary magnetic field (IMF) components	Provides upstream solar wind condition at Sun-Earth Lagrange Point 1 (L1) to run the NAIRAS model
DSCOVR Faraday Cup and Magnetometer	Solar wind velocity, density, and IMF components	Provides upstream solar wind condition at L1 to run the NAIRAS model
GOES Energetic Particle Sensor	Differential and integral charged particle flux	Derives the incident solar energetic particles (SEP) spectral fluence rates for the NAIRAS model

The team used the NAIRAS model for both global radiation data and radiation over specific flight paths. To output global data, the model requires the user to input the specific date for the data of interest. Alternatively, for radiation data on specific flight trajectories, the user needs to upload a file of the flight trajectory details including the location, altitude, and time. The flight trajectory information was extracted from FlightAware, which is a flight tracking system. The team copied individual flight data from the website and formatted it into a text file that would be a valid input for the NAIRAS model. The model processing took several days and calculated radiation dosages for each individual flight path.

The NAIRAS model outputs data in a zipped folder, which contains radiation levels for SEPs, GCRs, and total doses along with the corresponding latitudes, longitudes, and altitudes. Some key output variables include hourly-averaged total effective radiation dose rates, silicon absorbed dose rate, and tissue absorbed dose rate. The model is capable of outputting data with a spatial resolution of 1° latitude/longitude and covers altitudes from 0 – 90 km. Time metadata that corresponds to all the outputted data can be found in one singular file in the downloadable zipped data folder.

2.2 Data Processing

Using Python 3.13 code developed by science advisor Dr. Guillaume Gronoff, the team processed the hourly data files for every day of the three geomagnetic storms. All radiation variables were in the correct units and did not need conversions. The extracted radiation data were plotted on 2D Mercator map projections to provide a visual format that pilots were familiar with. The global visualizations were first produced for APA's broader goals. These maps were created using hourly averaged data over all latitudes and longitudes for a singular altitude. Global maps were created for each altitude between 8 km to 15 km for aviation purposes, but 20 km was also plotted simply to emphasize the drastic and non-linear increase in radiation at much higher altitudes.

The same principle was applied to the North Atlantic study area, and the scope of the maps was narrowed using Python. The latitude range was limited from 40° N to 70° N degrees and the longitude range from 90° W to 10° E. This longitude range roughly encompasses the eastern half of the United States (starting from around Wisconsin) and goes past the Atlantic Ocean and into Europe (ending around Frankfurt, Germany). From the NAIRAS output data folder, the effective dose rate measured in micro sieverts (μSv) was extracted, as this is the most appropriate unit of radiation for the partner organization to use for decision-making. The effective dose is a value representative of radiation for the whole body and includes the sensitivity of individual organs to different types of radiation.

In addition to static maps, animated Graphics Interchange Format (GIF) files were produced to visualize the change in radiation dose over time (hourly) and over different altitudes. Specific flight paths were overlaid on the radiation environments to better visualize potential routes for pilots and our partner organization.

2.3 Data Analysis

The team conducted quantitative analyses to better illustrate the changes in radiation for commercial pilots' experience. For all three space weather events, the team used total dose data from the DAT files to compute the mean total effective radiation dose rate at 70° latitude averaged across a longitudinal range from 90° W to 10° E. The mean was computed over a 24-hour period, which roughly matched the duration of the space weather events, at individual altitudes ranging from 8 km to 15 km to cover the typical range of commercial aviation. Although most transatlantic flights are much shorter, the 24-hour mean is still representative of the probable radiation exposure during the radiation event. A generalized percent decrease formula shown in Equation 1 was used to calculate the change in radiation between altitudes. With this quantitative analysis, pilots can better understand the variation in radiation for aviation safety.

$$\frac{\text{higher altitude dose} - \text{lower altitude dose}}{\text{higher altitude dose}} \times 100\% \quad (1)$$

The maximum and minimum values were also computed for every hour in this region as requested by the APA to assess the highest and lowest possible risk of exposure to radiation.

3. Results

3.1 Analysis of Results

Plotting the total effective dose rates for all three storms revealed important details about radiation at commercial aviation altitudes. The Mercator map projections in this section all have longitude on the x-axis and latitude on the y-axis while the total effective dose rate is represented by the color on the map. Colors that are closer to red indicate higher radiation levels and colors closer to blue are representative of lower effective dose rates. The color bar shows specific values for different colors for a more precise reference. The black discrete line present in some of the maps represents a 20 µSv/h threshold that the APA uses as a guideline for staying within safe radiation exposure levels. Areas above the line exceed this recommended threshold.

3.1.1. October 28-30th 2003 Storm

The Halloween 2003 Storm lasted multiple days from late October 2003 into early November 2003 and reached the maximum G5 grade for a geomagnetic storm. For this case study, the focus was on the beginning of the storm, from October 28th - 30th, as it contained three peaks, a rapid decrease in the observed GCR intensity that follows a coronal mass ejection (namely Forbush rapid decrease), in the observed GCR intensity that follows a coronal mass ejection (namely Forbush decrease), an example of magnetic field weakening, and the overall storm peak. The overall storm peak occurred from 23:00 UT to 00:00 UT between the 28th and 29th, though the maximum dose rate was only 23.7 µSv/h at 12 km. Much of the surrounding hours also had elevated radiation levels with a first peak occurring between 15:00 UT and 16:00 UT on the 28th and reaching 20.9 µSv/h but not maintaining over 20 µSv/h between peaks. The third and final peak of the case study period of this event came on the 29th from 22:00 UT to 23:00 UT and lasted into the early morning of the 30th (Figure 2).

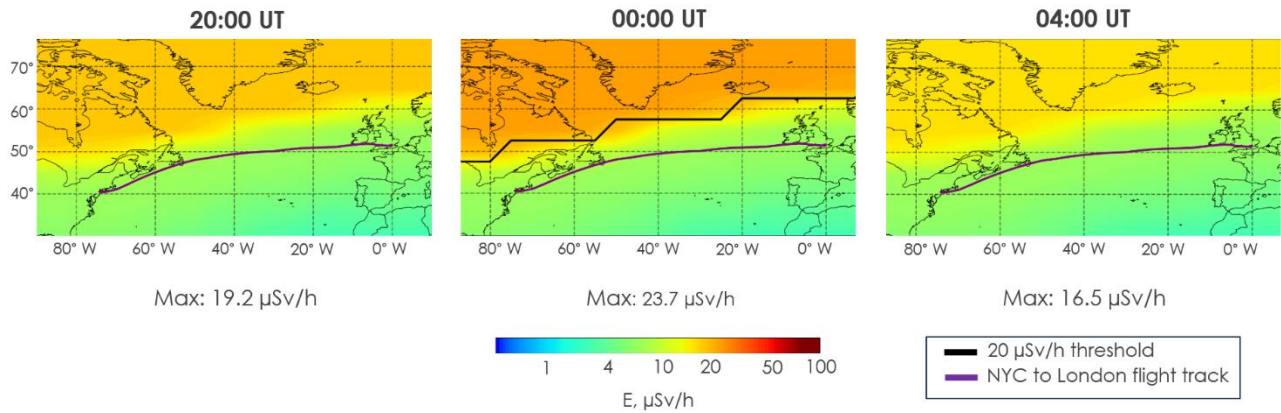


Figure 2: Regional total effective dose rate for October 28-29, 2003, before, during, and after storm peak at 12 km (FL390)

For the first two peaks, areas of enhanced radiation remained north of most NYC to London flight paths. This is because the ring current had not charged yet, which meant a near full strength magnetic field provided ample shielding. After those peaks cleared, the ring current charged sufficiently which allowed the third peak, although notably weaker, it reaches much further south, into the flight path (see appendix A for comparison). Part of the reason for this being weaker than previous peaks was an ongoing Forbush decrease. In the quiet time before the first increase on the 28th, the GCR radiation was around 6 $\mu\text{Sv/h}$, but in the quiet time before and after the third peak, the GCR radiation was around 4 $\mu\text{Sv/h}$. Given a 2 $\mu\text{Sv/h}$ decrease is 10% of the recommended limit, this is a notable reduction in radiation.

Vertical radiation profiles spanning a flight path from New York City to London display the radiation environment at altitudes ranging from Earth's surface to 20 km. Profiles of the total effective radiation dose levels reinforce how critical altitude is for flights and gives end users a better idea of how close flight routes can be to high levels of radiation. These plots were produced using NAIRAS TED rate data and processed in Python to show the changing radiation levels over a flight trajectory from New York City to London. Radiation levels in the vertical profile became greater as the flight increased in elevation (Appendix figure C1).

3.1.2. January 20th, 2005 Storm

The 2005 storm occurred on a single day, with the most notable changes in the radiation environment occurring from 04:00 UT to 14:00 UT. Figure 3 depicts most of this timeframe, with time stamps at 04:00 UT, 07:00 UT, and 10:00 UT. Within the span of three hours, the TED rate increased from 5.8 $\mu\text{Sv/h}$ to 93.5 $\mu\text{Sv/h}$ at an altitude of 12 km, which is a very common cruising altitude for commercial aviation. At the storm maximum which occurred at 07:00 UT, the 20 $\mu\text{Sv/h}$ threshold intersected with the example flight path from New York City to London, indicating that pilots and air crew would be exceeding the recommended radiation exposure level. A few hours after the storm's maximum, at 10:00 UT, the TED rates were elevated, although the threshold shifted north and was no longer intersecting with the flight path.

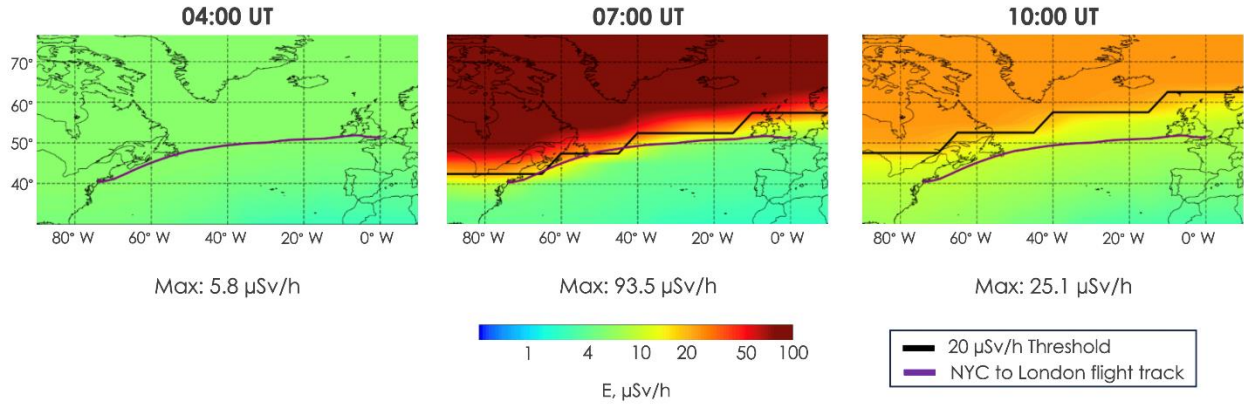


Figure 3: Regional total effective dose rate for January 20th, 2005, before, during, and after storm peak at 12 km (FL390)

Figure 4 depicts how the radiation environment changed with altitude, with maps showing the study area at 8 km, 10 km, and 12 km altitudes during the storm maximum that occurred at 07:00 UT. These altitudes encompass the lower and upper bounds of common cruising altitude for commercial flights. At 8 kilometers, the TED rate was relatively low when compared to the higher altitudes and there was no area on the map that exceeded the 20 $\mu\text{Sv/h}$ threshold. At 10 kilometers, the TED rate was notably higher, with a 44.8 $\mu\text{Sv/h}$ maximum measurement. Although the threshold line was present at this point, it did not intersect with the example flight track. At 12 kilometers the threshold was further south and intersected with the flight track. The maximum observed TED rate at this altitude was 93.5 $\mu\text{Sv/h}$, over two times higher than the 10-kilometer step. Vertical dose plots (Figure 5) show the radiation environment and severe levels crossing the flight path from NYC to London.

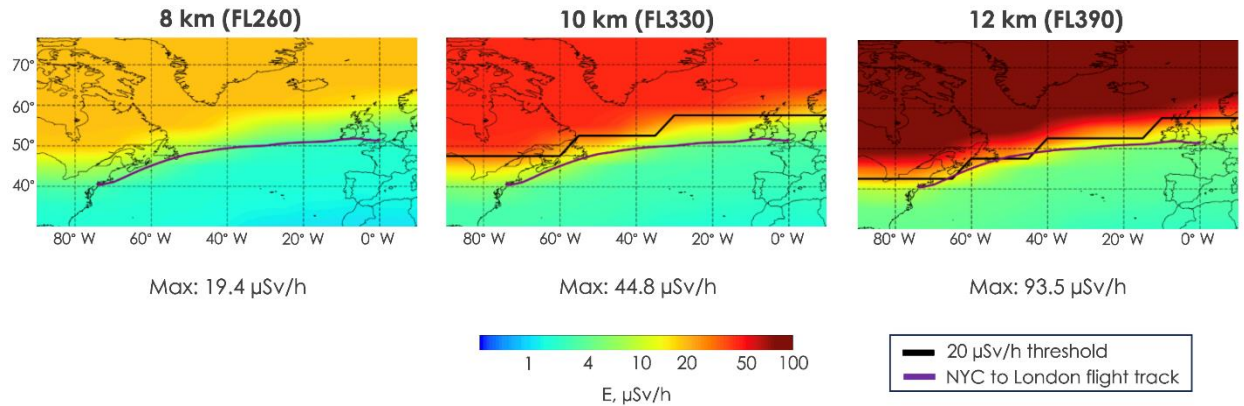


Figure 4: Regional total effective dose rate for January 20th, 2005, at 07:00 UT for three altitudes

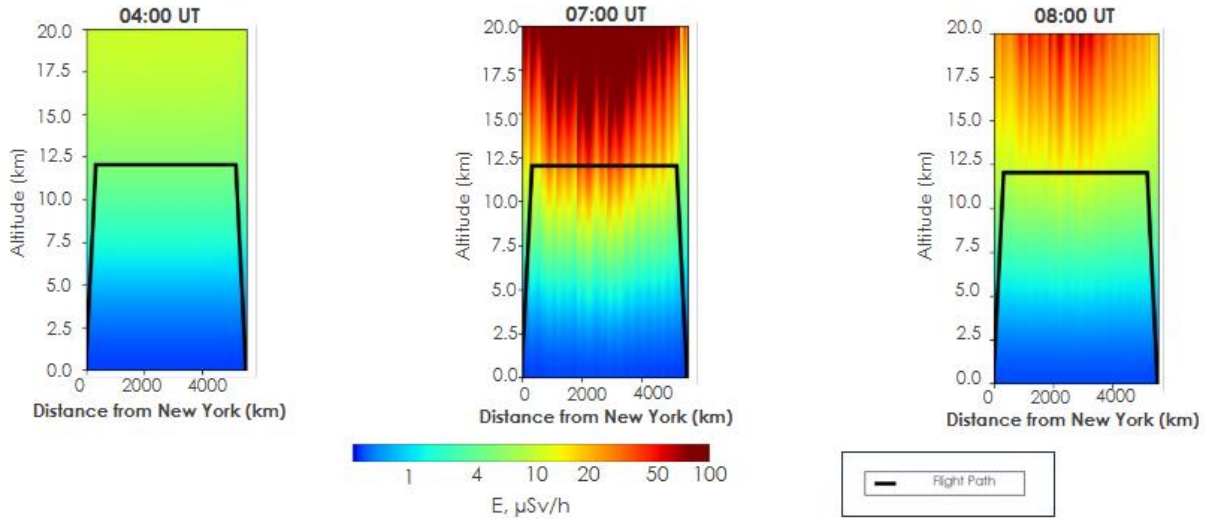


Figure 5: Vertical TED profile for the January 20th, 2005 storm for three timestamps, corresponding with the time stamps from figure

3.1.3. May 10-11th, 2024 Storm

The Gannon storm yielded different results for radiation exposure than the previous two storms. Figure 6 depicts the variation of the radiation on May 10th, with the radiation increasing from 7.6 $\mu\text{Sv/h}$ to 8.1 $\mu\text{Sv/h}$ and then back down to 5.5 $\mu\text{Sv/h}$. There was a very slight increase in radiation over the duration of the day, but the TED rate did not reach the 20 $\mu\text{Sv/h}$ threshold that was seen in the previous two storms.

Furthermore, the radiation increased slowly over the entire day and the NYC to London track was not in a high radiation environment.

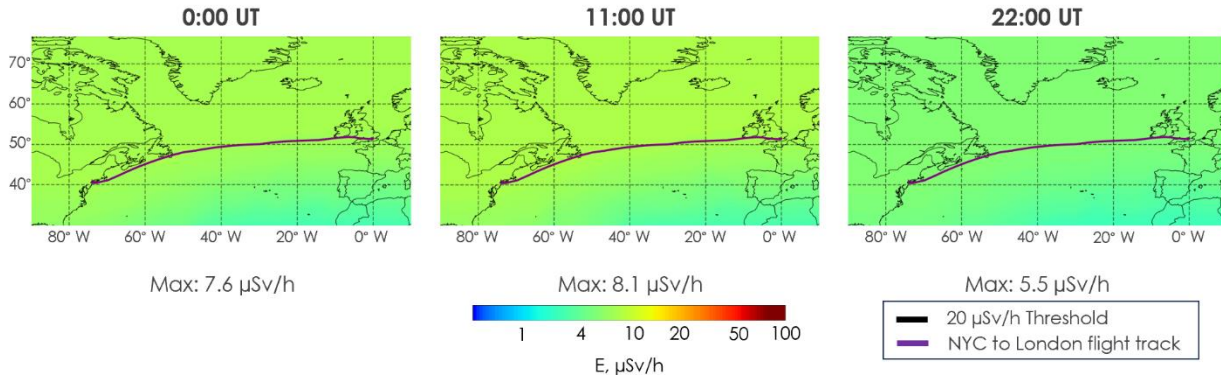


Figure 6: Regional total effective dose rate for May 10th, 2024 for three timestamps at 12 km (FL390)

Figure 7 shows the radiation environment on May 10th for different altitudes and a similar trend can be seen as in the previous storms with the radiation increasing with altitude. However, the TED rates were not at significant levels with the maximum at 12 km (FL390) only at 8.1 $\mu\text{Sv/h}$ which was still below the 20 $\mu\text{Sv/h}$ threshold. For May 10th, during the storm, the radiation environment did not reach high levels at aviation altitudes.

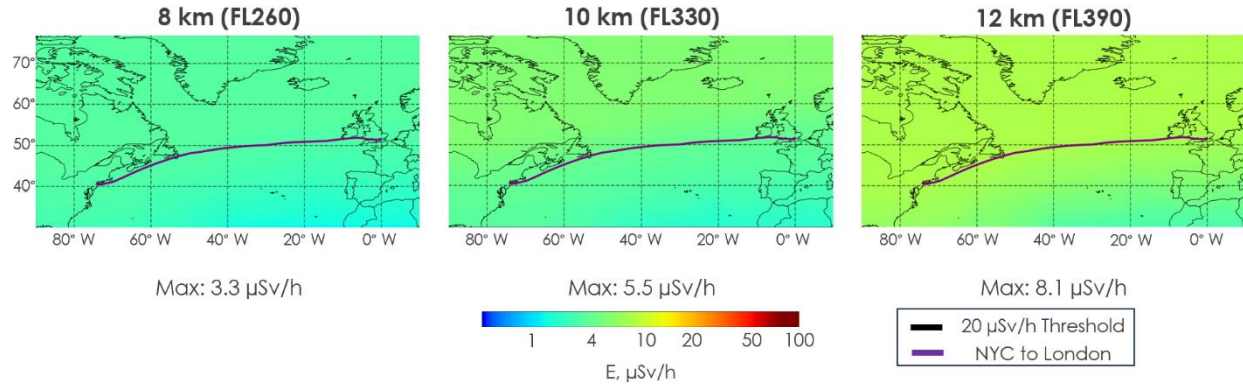


Figure 7: Regional total effective dose rate for May 10th, 2024 at 11:00 UT for 3 altitudes

In addition to the figures from May 10th, Figure B1 in the appendix depicts the TEDTED rate for several timestamps on May 11th. The radiation started increasing around 00:00 UT on May 11th, going from 5.5 $\mu\text{Sv/h}$ to 8.6 $\mu\text{Sv/h}$ in the span of 6 hours. The radiation peaked at 06:00 UT but the TED rate was only 8.6 $\mu\text{Sv/h}$. Unlike the previous two storms, the TED rate did not reach the 20 $\mu\text{Sv/h}$ threshold throughout the storm, meaning pilots and aircrews were not exposed to unsafe amounts of radiation in the North Atlantic region.

The TED rate was also studied at different altitudes during the peak of the radiation exposure. As seen in Figure B2, in the appendix, the radiation at 8 km (FL260) had a low value of 3.1 $\mu\text{Sv/h}$, increased to 5.3 $\mu\text{Sv/h}$ at 10 km (FL330), and to 8.6 $\mu\text{Sv/h}$ at 12 km (FL390). Overall, the radiation increased by 5.5 $\mu\text{Sv/h}$ from the lower end (8 km) to upper end (12 km) of aviation altitudes. This is equivalent to a 64% decrease in TED rates when decreasing altitude from 12 km to 8 km, but it is important note that the maximum TED rate of 8.6 $\mu\text{Sv/h}$ was still well below the 20 $\mu\text{Sv/h}$ threshold used by the APA. This is equivalent to a 64% decrease in TED rates when decreasing altitude from 12 km to 8 km, but it is important note that the maximum TED rate of 8.6 $\mu\text{Sv/h}$ was still well below the 20 $\mu\text{Sv/h}$ threshold used by the APA.

Vertical plots of the TED further illustrate (Figure C2) the proximity of the flight path to the elevated radiation levels. These plots show the TED levels over the duration of the storm, and emphasize how far into the atmosphere radiation can reach, despite the weaker levels in this particular case study.

In addition to the regional plots and vertical radiation profiles, preliminary quantitative analysis was completed to understand variations in radiation with altitude. For this analysis, the average of the TED rate was taken over a period of 24 hours for latitude 70° N and averaged over a longitude range of 90° W to 10° E. This was done to understand how radiation levels are at higher latitudes during space weather events. As seen in Table 2, for January 20th, there was a 12.02 $\mu\text{Sv/h}$ decrease in average effective dose rate going from 16.69 $\mu\text{Sv/h}$ at 12 km to 4.67 $\mu\text{Sv/h}$ at 8 km. The 12.02 $\mu\text{Sv/h}$ change corresponds to about a 72% decrease in radiation going from 12 km to 8 km.

Table 2

Maximum, Minimum, and Mean Total Effective Dose Rates for January 20th, 2005

Altitude	Latitude	Longitude	Max Dose Rate ($\mu\text{Sv/h}$)	Min Dose Rate ($\mu\text{Sv/h}$)	Mean Effective Dose Rate ($\mu\text{Sv/h}$)
12 km	70° N	90° W to 10° E	93.48	5.569	16.69
11 km	70° N	90° W to 10° E	64.63	4.723	12.37
10 km	70° N	90° W to 10° E	44.79	3.888	9.14
9 km	70° N	90° W to 10° E	30.3	3.112	6.63
8 km	70° N	90° W to 10° E	19.39	2.422	4.67

Similar analyses were done for the 2003 and 2024 events as seen in Appendix D. For the 2003 storm, there was around a 71% decrease in average total effective dose rate when going from 12 km to 8 km altitude. Unlike the 2003 and 2005 events, May 11th, 2024 showed a 61% decrease in radiation when dropping 4 km in altitude. It is also important to note that the individual radiation values for May 11th were significantly lower than the values for 2003 and 2005.

3.2 Errors & Uncertainties

The spatiotemporal resolution of the NAIRAS model was the first limitation of this study. Currently NAIRAS modeled output data can only be downloaded at 5-degree longitude by 2.5-degree latitude resolution from CCMC, despite the model having 1 degree longitude by 11 degree latitude resolution capabilities. This was done by CCMC to reduce data load. It is notable to add that any forecast and nowcast data will also be in this coarser resolution, so it is consistent. Data was collected in hourly intervals, also to save storage. This may have led to some distortion of when storm peak occurred if it started in the later part of an hour.

NAIRAS data have been validated by many dosimeters, both via aircraft and balloon. The primary means of validation is the ARMAS (Automated Radiation Measurements for Aerospace Safety) FM5 (Flight Module 5), which can be flown on aircraft to measure in-situ airborne radiation. However, it has a margin of error of 30%. While the NAIRAS falls within this, it is currently impossible to further validate the model data. Also, no validation mission has flown during an SEP event, making this data's margin of error somewhat unknown (Mertens et al. 2025).

Another uncertainty included the input for the NAIRAS model. After 2020, the GOES alpha differential flux data used as an input for the NAIRAS model is unreliable. On CCMC, users can choose whether to use SEP heavy ions and protons for the model or only protons. Due to the unreliability of GOES alpha differential flux after 2020, only the protons should be selected for SEP for any date after March 4, 2020. If protons and heavy ions were selected, incorrect data from the GOES satellites would skew results and show much larger values. Therefore, it is important to note the May 2024 Gannon Storm is run without heavy ions, while the two other storms include heavy ions. Fortunately, the TED data is not strongly impacted by heavy ions at aviation altitudes, especially considering the Gannon Storm produced comparatively weaker radiation values.

The outcomes of his study were limited by its ten-week timeframe. As a result, further analysis of other radiation events should be conducted to support its conclusions and confirm the findings. More case studies are needed, particularly of storms that are strong radiationally, not necessarily geomagnetically, like January 2005, to better understand these isolated events. Other studies to measure radiation levels at quiet times are needed to better understand base-levels of radiation and standard non-storm risk levels.

4. Conclusions

4.1 Interpretation of Results

Through this study, the team found that the NAIRAS model provides the necessary data to map radiation environments over the North Atlantic region, as well as globally. The model returned TED data, which allowed the team to complete radiation maps, vertical profiles and quantitative analysis to better understand the radiation environment. In the process of mapping, the team found that the TED rate is generally greater at higher latitudes. However, the dose rate is not consistent across the same latitude due to the offset between the geomagnetic and geographic poles. These results are significant because they showed that the 20 $\mu\text{Sv/h}$ threshold is lower in latitude over North America than it is over Europe. This inconsistent shielding across the same latitude is a prominent feature in the observed case studies and is key in understanding the radiation environment. This feature may not be intuitive and so is an important point of education and consideration for flight planning.

For this high latitude study area, the TED rates decrease as the altitude decreases. For the observed storms, there was about a 20% decrease in radiation with each kilometer step down in altitude. Across commercial aviation cruising altitudes, 12 km to 8 km, the decrease was over 70% for the strong SEP events, Halloween 2003 and January 20, 2005, with January having a slightly larger reduction in radiation than Halloween. The Gannon storm only saw about a 61% reduction across the same altitudes but still showed a significant decrease in radiation over a change in altitude.

The radiation exposure can go from standard rates to heightened levels within the duration of a single transatlantic flight. This can occur due to strong radiation getting through some of the weaker magnetic field protection and penetrating into the Earth's atmosphere, or the duration of a storm can be long enough that the magnetic field weakens sufficiently to shift south of the North Atlantic tracks, leaving them exposed. Because of this and the tilt of the geomagnetic poles, the North Atlantic flight tracks are an important area of study.

4.2 Feasibility & Partner Implementation

The NAIRAS model was found to be an effective tool for visualizing the radiation environment at aviation altitudes. Although its outputs are generally catered to the scientific community, the team was able to format the NAIRAS data to fit pilots' needs. This included changing the polar views from the NAIRAS model to Mercator map projections which are more easily understood by pilots and a more general audience. Furthermore, total effective dosage data from NAIRAS was put into tables in an organized manner for the partners to better understand the exact quantitative doses that pilots may receive during radiation storms. Adding flight tracks to the radiation maps allowed for better understanding of TED rates for specific flight paths in the North Atlantic region. Overall, this project highlighted the transition from scientific data to digestible information for the pilots and public. The APA is also planning to present some of the work done here to a larger audience and educate them on radiation exposure at commercial aviation altitudes.

Currently, the NAIRAS model does not have forecasting options through CCMC, but it will soon be available. With the forecasting option, the radiation environment can be predicted up to 7 hours into the future. This will allow pilots to include radiation concerns into their flight planning. The goal is to have space weather and radiation integrated into aviation systems similar to how terrestrial weather is integrated now. Overall, these developments show that scientific radiation models like NAIRAS can be adapted for operational use, making it possible for pilots to factor radiation into their decision-making.

5. Acknowledgements

The North Atlantic Space Weather team would like to thank Dr. Xia Cai (NASA Langley Research Center), Dr. Christopher Mertens (NASA Langley Research Center), Dr. Guillaume Gronoff (NASA Langley Research Center) and Dr. Daniel Phoenix (NASA Langley Research Center) for their invaluable science advising, Laramie Plott (Virginia – Langley), Brent Bowler (Virginia – Langley), Brooklyn Appling (Virginia – Langley), Jennifer Hall (Virginia – Langley), Jack Graziano (Virginia – Langley), Jamie Favors (NASA Headquarters) and Alyson Bergamini (Analytical Mechanics Associates) for their programmatic support, and the Allied Pilots Association project partners Captain Rondeau Flynn and Captain Kevin Macelhaney for their enthusiasm, feedback and support throughout the project term.

Any opinions, findings, and conclusions or recommendations expressed in this material are those of the author(s) and do not necessarily reflect the views of the National Aeronautics and Space Administration.

This material is based upon work supported by NASA through contract 80LARC23FA024.

6. Glossary

CCMC – NASA Community Coordinated Modeling Center at Goddard Space Flight Center

Cutoff Rigidity – shielding that the Earth’s magnetic field provides from high energy particles

Earth observations – Satellites and sensors that collect information about the Earth’s physical, chemical, and biological systems over space and time

Flight Path – planned trajectories flights travel along

Forbush Decrease – a rapid decrease in the observed GCR intensity that follows a coronal mass ejection (CME)

GCR – galactic cosmic rays

NAIRAS – Nowcast of Aerospace Ionizing RAdiation System

Neutron Monitor – ground-based detector that measures the number of high-energy charged particles in the Earth’s atmosphere

Ring Current – an electric current carried by charged particles that are trapped in Earth’s magnetosphere

SEP – solar energetic particles

Sievert – unit in the International System of Units (SI) for measuring the biological effect of ionizing radiation

Solar Wind Speed – the speed at which the solar wind particles travel through space

TED – total effective dose (rate)

Transatlantic – the area that crosses the Atlantic Ocean

7. References

Allied Pilots Association. (2023). Alliedpilots.org. <https://www.alliedpilots.org/Public-Pages/Public/About>

Harvard Health Publishing. (2021, September 30). Radiation Risk from Medical Imaging. Harvard Health; Harvard Health. <https://www.health.harvard.edu/cancer/radiation-risk-from-medical-imaging>

Jun, I., Garrett, H., Kim, W., Zheng, Y., Fung, S. F., Corti, C., Ganushkina, N., Gou, J. (2024). A review on radiation environment pathways to impacts: Radiation effects, relevant empirical environment models, and future needs. *Advances in Space Research*. <https://doi.org/10.1016/j.asr.2024.03.079>

Langner, I., Blettner, M., Gundestrup, M., Storm, H., Aspholm, R., Anssi Auvinen, Eero Pukkala, Georg Philipp Hammer, Zeeb, H., Hrafnkelsson, J., Vilhjalmur Rafnsson, Hrafn Tulinius, G. de Angelis, Verdecchia, A., Tor Haldorsen, Tveten, U., Harald Eliasch, Hammar, N., & Linnarsjö, A. (2003). Cosmic radiation and cancer mortality among airline pilots: Results from a European cohort study (ESCAPE). *Radiation and Environmental Biophysics*, 42(4), 247–256. <https://doi.org/10.1007/s00411-003-0214-7>

Mertens, C., Wilson, J., Blattnig, S., Kress, B., Norbury, J., Wiltberger, M., Solomon, S., Tobiska, W., & Murray, J. (2008). Influence of space weather on aircraft ionizing radiation exposure. *46th ALAA Aerospace Sciences Meeting and Exhibit*. <https://doi.org/10.2514/6.2008-463>

Mertens, C.J., Kress, B.T., Wiltberger, M., Blattnig, S.R., Slaba, T.S., Solomon, S.C., Engel, M.(2010). Geomagnetic influence on aircraft radiation exposure during a solar energetic particle event in October 2003. *Space Weather*, 8(3). <https://doi.org/10.1029/2009SW000487>

Mertens, C. J., Gronoff, G. P., & Phoenix, D. B. (2025). NAIRAS version 3 atmospheric ionizing radiation validation: Comparisons to RaD-X measurements. *Space Weather*, 23, e2024SW004296. <https://doi.org/10.1029/2024SW004296>

- Wan, Z., Hook, S., & Hulley, G. (2021). *MODIS/Terra Land Surface Temperature/Emissivity Daily L3 Global 1km SIN Grid (V061)* [Data set]. NASA EOSDIS Land Processes DAAC. Retrieved January 20, 2022, from <https://doi.org/10.5067/MODIS/MOD11A1.061>
- Xue, D., Wu, L., Xu, T., Wu, C., Wang, Z., & He, Z. (2024). Space weather effects on transportation systems: a review of current understanding and future outlook. *Space Weather*, 22(12). <https://doi.org/10.1029/2024sw004055>

8. Appendices

Appendix A: Regional Plots of Total Effective Dose for October 2003 Storm

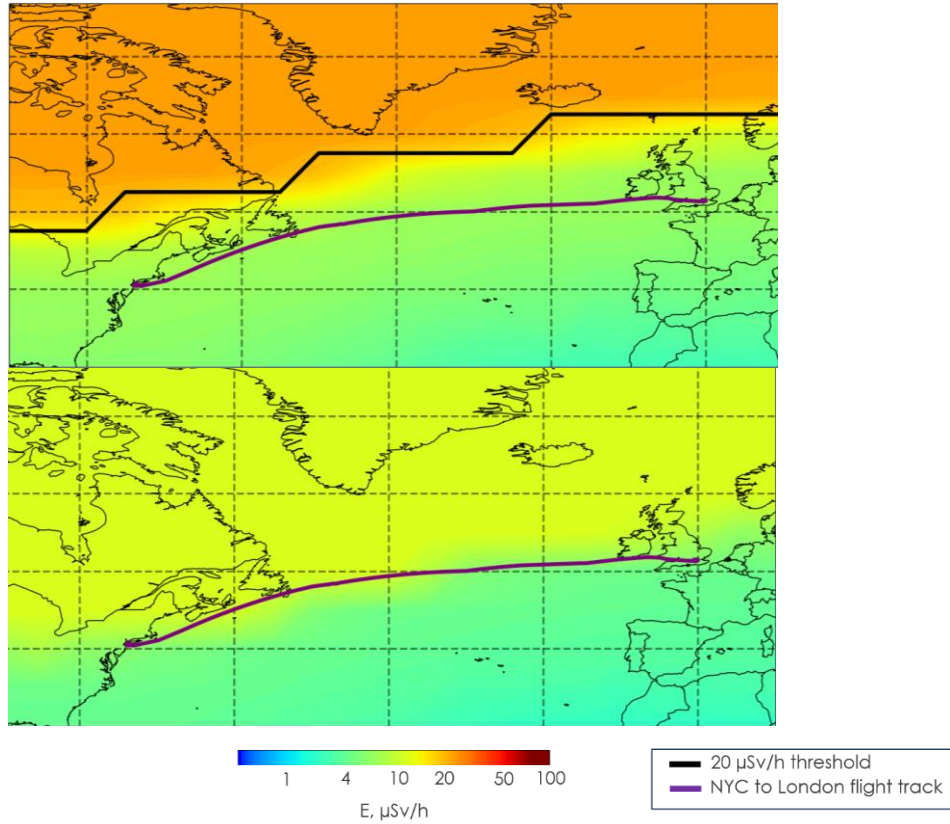


Figure A1: Regional total effective dose rate for October 29th, 2003, at second peak (top) and third peak (bottom) at 12 km (FL390)

Appendix B: Regional TED plots for May 11th, 2024

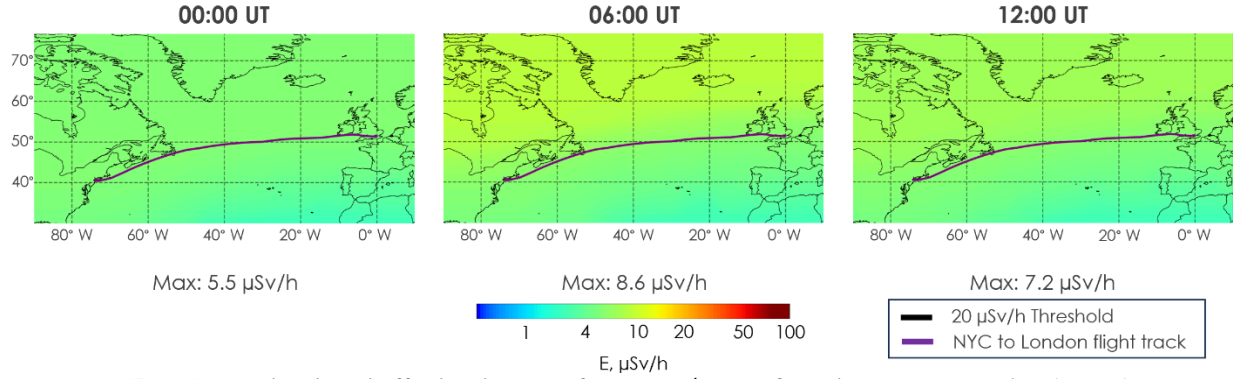


Figure B1: Regional total effective dose rate for May 11th, 2024 for 3 timestamps at 12 km (FL390)

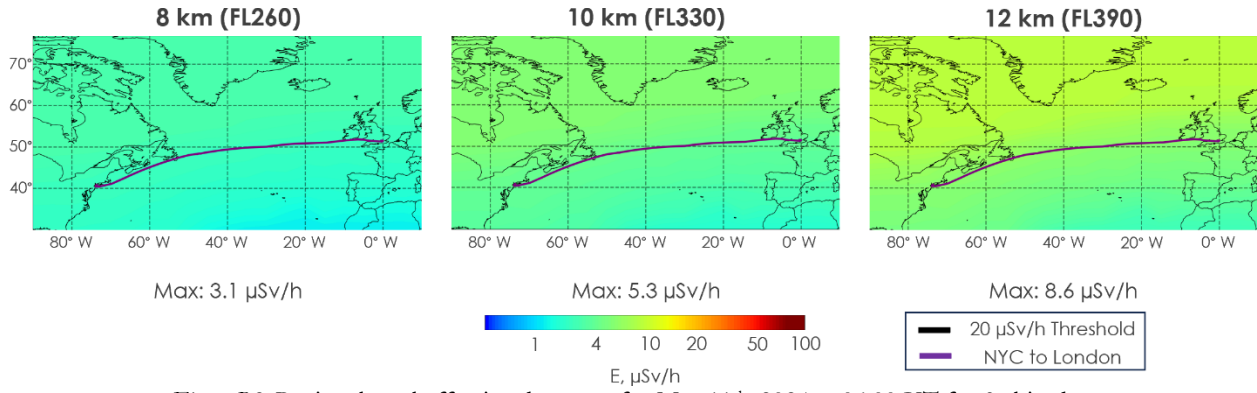


Figure B2: Regional total effective dose rate for May 11th, 2024 at 06:00 UT for 3 altitudes

Appendix C: Vertical Radiation Profiles for Flight Paths

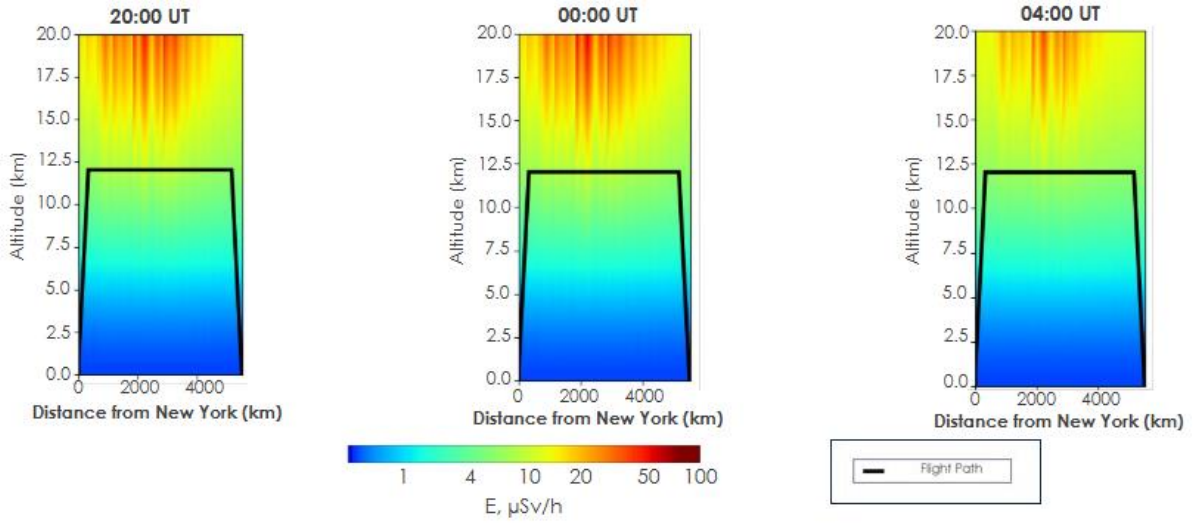


Figure C1: Vertical radiation profile for the Halloween storm, October 28th, 2003

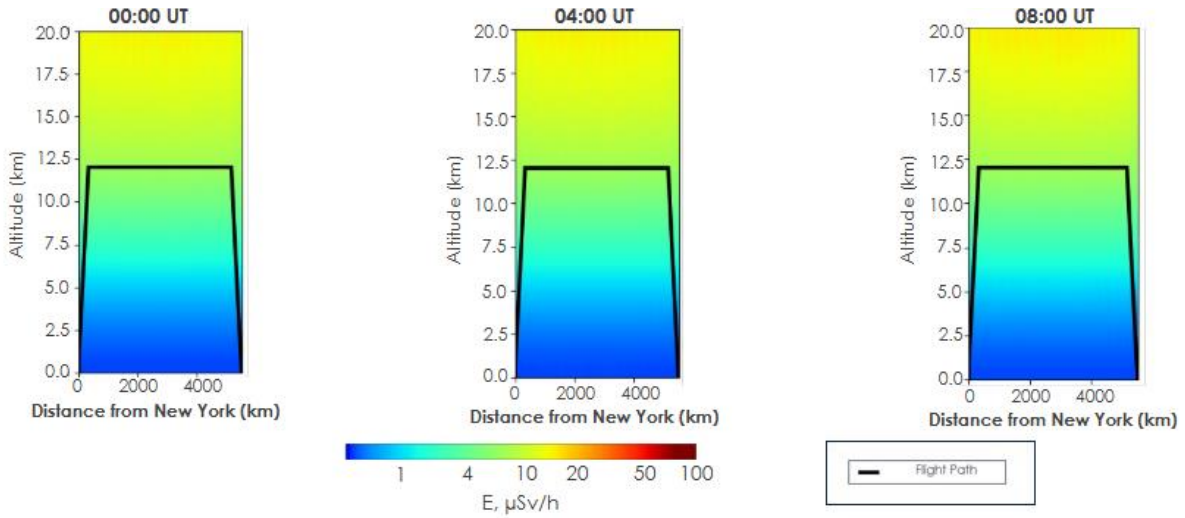


Figure C2: Vertical radiation profile for the May 11th, 2024 storm

Appendix D: Quantitative Analysis of TED Rates

Table D1

Maximum, Minimum, and Mean Total Effective Dose Rates for October 29th, 2003

Altitude	Latitude	Longitude	Max Dose Rate (μSv/h)	Min Dose Rate (μSv/h)	Mean Effective Dose Rate (μSv/h)
12 km	70° N	90° W to 10° E	23.72	4.23	10.11
11 km	70° N	90° W to 10° E	15.91	3.57	7.27
10 km	70° N	90° W to 10° E	10.82	2.94	5.31
9 km	70° N	90° W to 10° E	7.34	2.37	3.88
8 km	70° N	90° W to 10° E	4.90	1.85	2.80

Table D2

Maximum, Minimum, and Mean Total Effective Dose Rates for May 11th, 2024

Altitude	Latitude	Longitude	Max Dose Rate (μSv/h)	Min Dose Rate (μSv/h)	Mean Effective Dose Rate (μSv/h)
12 km	70° N	90° W to 10° E	8.58	5.47	7.01
11 km	70° N	90° W to 10° E	6.81	4.64	5.72
10 km	70° N	90° W to 10° E	5.34	3.82	4.58
9 km	70° N	90° W to 10° E	4.10	3.07	3.59
8 km	70° N	90° W to 10° E	3.08	2.39	2.73